6ICEGE
6th International Conference on Earthquake Geotechnical Engineering
1-4 November 2015
Christchurch, New Zealand

# Large embankments in near-source areas

A. Dello Russo[1], S. Sica[2]

## ABSTRACT

The objective of the numerical study is to investigate the peculiarities of near-source seismic propagation and to evaluate its effects on the seismic response of large embankments. The seismic response of such earth structures may be strongly influenced by spatial variability and asynchronism of the ground motion. In the case of large dams cracks in the watertightness element may be thus promoted. In the study the reference rock formation and the earthquake source are part of the model together with the soil deposit and the embankment. The source has been simulated by introducing an interface within the rock and assigning to the rupture points, along the fault, the motions defined through suitable mathematical laws derived from the seismology.

## Introduction

Accelerometric and velocimetric recordings acquired in different sites located at short distances from seismic sources, during several earthquakes worldwide have shown the variability of seismic motion characteristics in near-source conditions. In particular, in the vicinity of the seismic source the presence of a bimodal spectral shape on at least one of the components of motion was observed (Somerville, 2005). A significant energy content at high frequencies is observed, due to minor dissipation occurring during the short wave path from the seismic source and the site. The spectral peak at low frequencies, however, is probably caused by the presence of an impulsive component induced by the phenomenon of “forward directivity” (Somerville, 2005). Other typical characteristics of the near-source seismic motion are: the presence of residual displacements at the ground level, or evidence of the fault on the surface ("fling-step"); high PGA, PGV and PGD values compared to those recorded far from the source (far-field conditions) for earthquakes with the same magnitude; the presence of a non-negligible vertical motion, with reference to the horizontal components; the almost simultaneous arrival of S and P waves due to the short source-site distance; further P and S waves contribute to both horizontal and vertical motions because the wave front approaches the free surface with an inclination which can be very different from the sub-vertical (as it happens for sites far from the focal mechanism). Finally, the frequency content of the signal depends on the focal mechanism, i.e. geometry and direction of fracture propagation, slip map and source-site relative position.

In geotechnical earthquake engineering, it is particularly important to characterize both the frequency content of the seismic signal and its asynchronism along the bedrock roof. The seismic response of large structures characterised by predominant longitudinal development (dams, road

[1]PhD, Department of Engineering, University of Sannio, Benevento, Italy, angelodr@unisannio.it
[2]Assistant Professor, University of Sannio, Benevento, Italy, stefsica@unisannio.it

embankments, tunnels, bridges, pipelines) can be significantly influenced by kinematic and dynamic effects of the near-source wave propagation. The asynchronism of the seismic motion at the base of an earth embankment, for example, may induce unsafe stresses and deformations. The note illustrates a study on the seismic motion induced in near source conditions at the base of embankments (for simplicity, reference is made to a typical section), for different positions of the structure with respect to the location and size of the rupture zone.

## Numerical model

In modelling problems of geotechnical earthquake engineering, the subsoil borders generally coincide with the bedrock roof, which is excited by a single seismic input motion. In this study, for taking into account the peculiarities of the near-source wave propagation, the geometric model is considerably wider, as it includes the seismic source, and requires the simulation of the focal mechanism and wave propagation (Figure 1).

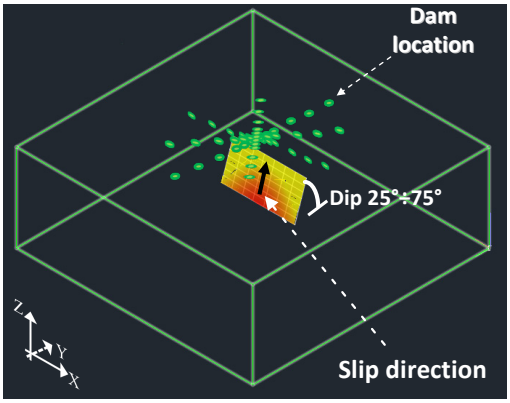


Figure 1. 3D source model with all possible locations (green points) of the embankment

A three-dimensional model has been analysed, with plan dimensions of 200km x 200km and thickness of 20km. The subsoil is subdivided into two layers: the first, from the ground level down to a depth of 250m, is made up of silt and clay of medium consistency; the second is a rock resembling the rigid substratum. Above the ground surface an embankment is placed, whose geometrical features will be described in the following section. All the materials are characterised by a linear visco-elastic behaviour, with the exception of the interface between the two tectonic plates, where an elastic perfectly plastic mechanical model has been assigned. As regards the damping parameters, the Rayleigh formulation with one-frequency control has been used; in particular a damping, $\xi$, equal to 0.5% at the dominant frequency of about 0.025 Hz, was assigned at the bedrock, while a damping equal to 5% at the frequency of 0.40 Hz has been adopted for the soil and the earth dam layers. Tables 1 and 2 contain the values of the mechanical parameters characterizing the different materials of the model.

The system boundary conditions consist of absorbent surfaces according to the treatment proposed by Lysmer and Kuhlemeyer (1969). Finally, the size of the mesh elements has been calibrated as a function of the shear wave velocity of each material in order to properly simulate the development of body waves with a maximum frequency of 5 Hz. Around the fault area a

condensation of the mesh has been used. The propagation of the rupture is simulated during the analysis by accounting for equilibrium and congruence equations, failure criterion and constitutive model assigned to the fault region.

Table 1. Mechanical parameters of the different materials modelled.

| Zone | Density, $\rho$ ($kg/m^3$) | Poisson coeff., $\nu$ | S wave velocity, $V_S$ (m/s) | Damp. (%) |
|---|---|---|---|---|
| **Embankment** | 2000 | 0.30 | 430 | 5 |
| **Soil** | 1900 | 0.30 | 410 | 5 |
| **Rock** | 2750 | 0.20 | 2000 | 0.5 |

Table 2. Mechanical parameters of the material around the fault.

| Zone | $\rho$ ($kg/m^3$) | $\nu$ | $V_S$ (m/s) | Damping (%) | Cohesion (MPa) |
|---|---|---|---|---|---|
| **Fault** | 2600 | 0.20 | 635 | 0.5 | 150 |

***Source model***

Three different geometries of fault have been adopted (Figure 2), which are quite typical in Central and Southern Italy:

- *Fault 1*: width equal to 5 km, length of 6.5 km, enucleation point at 7 km below the ground level.
- *Fault 2*: width of 10 km, length of 17.5 km, enucleation point at 12 km below the ground level.
- *Fault 3*: width of 15 km, length of 25 km, enucleation point of 18 km below the ground level.

The angle of immersion of the faults ("dip") has been varied between 25° and 75°; the midpoint of the faults is located on the axis of the geometric model (Figure 2). Being the plan dimension of the source from case 1 to 3 increasing with depth, the associated magnitude will also be different. In particular, magnitude of 5.5, 6.25 and 6.5 for faults 1, 2 and 3 were respectively generated, according to Wells & Coppersmith equation (1994). The starting point of the rupture is the deepest point of the fault and the propagation occurs from left to right in Figure 2. The failure is a “second mode” mechanism, because the rupture occurs by sliding along the fault plane, with the rake (slip direction) parallel to the interface and the direction equal to the propagation of the rupture (Irwin, 1957).

To properly simulate the rupture process at the interface, for each node of the source a delay between the rupture initiation at the point of enucleation and the start of motion in the considered node was imposed. For the estimation of the delay-time, a velocity of rupture propagation ($V_{Rup}$) equal to 80% of the shear wave velocity of the rock was considered (Aki & Richards, 2002). In the analyses four different time histories of the velocity vector in the upper zone of the interface (fault) were hypothesized. The results here shown refer to the triangular function of the slip (Eq. 1), which produces high-frequency energy content at the source.

$$f_{(t)} = \begin{cases} \dfrac{2}{\alpha \cdot \tau^2} \cdot t & [0 \le t \le \alpha\tau] \text{ and } [0 \le \alpha \le 1] \\ \dfrac{2}{(1-\alpha) \cdot \tau^2} \cdot (\tau - t) & [\alpha\tau < t \le \tau] \text{ and } [0 \le \alpha \le 1] \\ 0 & [t < 0 \cup t > \tau] \end{cases} \quad (1)$$

In Eq. 1, $\tau$ is the duration of the rupture process to a single node (rise time). Each input node is also differentiated in terms of amplitude and duration of the rupture (Madariaga 1976), allowing a more realistic slip distribution on the extended source (decreasing slip-map with distance from the hypocenter).

The seismic wave generation at the source was simulated by a kinematic approach that consists of inserting a velocity function at each node of the source mesh. In each element the failure conditions are governed by the Tresca resistance criterion which is suitable to reproduce the mechanisms of a second-mode rupture (crisis for slipping plane). The assumption of elasto-plastic behaviour for the interface material has allowed to simulate the permanent deformations and especially to generate a content of higher frequencies, through the generation (local and temporary) of single plastic zones in the source volume. During the propagation of the rupture the sliding of the foot-wall of the fault is fixed to zero, by further internal constraints. These constraints are then removed during the subsequent stages of propagation of the wave front, avoiding abnormal reflections from the interface fault.

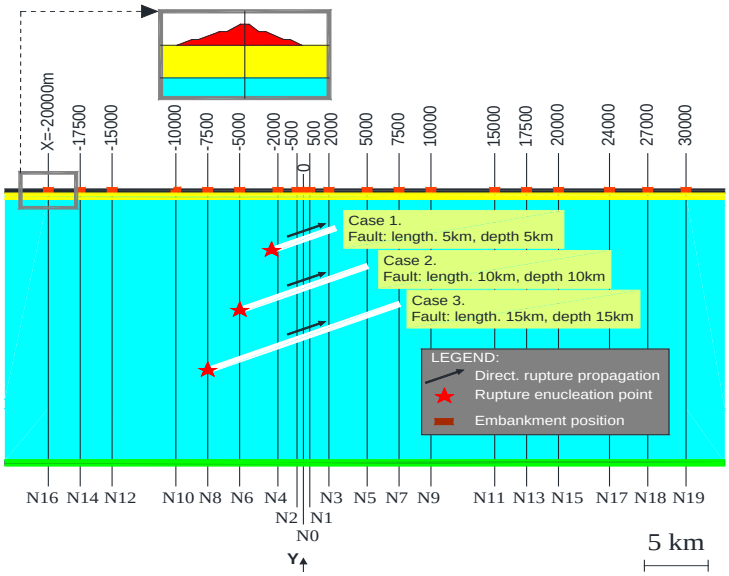


Figure 2. Different fault schemes (white segments) and embankment location along the free surface of the soil deposit. Central cross section (zy plane) of the scheme shown in Fig. 1

The results of a wide set of parametric 3D analyses show that the horizontal acceleration significantly decreases (by a rate of 50 to 70%) at a distance higher than 1.5 times the surface projection of the fault, where the near-field terms become negligible (Aki & Richards, 2002). Moreover, this distance tends to decrease as the depth of the fault increases (Fault 3).

### *Embankment model*

Embankments with different heights (20, 50 and 100 meters) and having a ratio between the maximum horizontal extent of the cross section and the height of about 6:1, have been analysed. In all cases, the length of the embankment is 1km long. In order to study the effect of the relative distance between the site (embankment) and the source (fault), the embankment location has been changed (with the fault in a fixed position) so that the structure is excited by the near-source or far-source seismic propagation. For both dam body and foundation soils, linear visco-elastic behaviour was considered (Table 1).

## Results

The results are shown with reference to (i) free-field ground motion and associated attenuation law and (ii) the effects of near-source seismic propagation on large embankments.

### *Attenuation laws in near-source conditions*

The proposed numerical model has been firstly adopted to develop attenuation relationships for predicting ground motion parameters characterizing the near-fault seismic propagation. At this stage, soil embankments were not included in the reference scheme of Figure 1. Attenuation relationships are necessary for the selection or generation of signals that can be adopted as input for site or building response analysis (time domain). Typical predictive relationships for characterizing pulse-like motion, typical of the near-source zone, have the following form:

$$\ln(PGV) = a + bM_W + c\ln(R^2 + d^2) + S \quad (2)$$

where PGV is the peak ground velocity, R is the planar source-site distance, $M_w$ is the moment magnitude, S encompasses site effects, *d* accounts for source depth and, finally, factors *a*, *b*, *c* are model parameters. Equation (2) can be adopted for both fault-normal and fault-parallel component of the motion. Large systems, such as dam embankments, may be much vulnerable to bi-directional shaking so that the fault-parallel component of the motion needs to be characterized too.

For each fault type (case 1 to 3) considered in this study (Figure 2), the obtained numerical predictions of PGV along the free surface of the model were compared to the values provided by the empirical attenuation law of Bray & Rodriguez-Marek (2004) for magnitude Mw varying between 5.5 and 6.5 (Figure 3). In Figure 3 indicators with different colour refer to different dip angles (darker indicators correspond to lower angles of dip). In addition, for a fixed distance, more values of PGV correspond to different sites (hypothetic seismic station), arranged radially with respect to the vertical axis of the source (Figure 1). It is possible to note that the comparison is quite satisfactory especially for higher values of magnitude (Figure 3b and 3c). In the latter case, all possible factors of variability exert a minor role with respect to earthquake magnitude and data scattering reduces.

$ln(PGV) = a + bM_w + cln(R^2 + d^2) + S$ The attenuation law by Bray & Rodriguez-Marek (2004) was obtained from a database of records for which a pulse-like waveform was identified or

observed on at least one of the two components of the ground motion. As well-known, this condition is related to the occurrence of directivity. In the reality the effects of forward-directivity might not occur because it is difficult to have a homogeneous slip map or a rupture direction parallel to the slip. For a fixed magnitude and angle of dip, the stations placed along the direction of propagation of the rupture (forward-directivity) have much higher values (even three times) than the stations at the same epicentral distance but positioned orthogonally or in the opposite direction to that of rupture propagation (neutral or backward directivity, respectively).

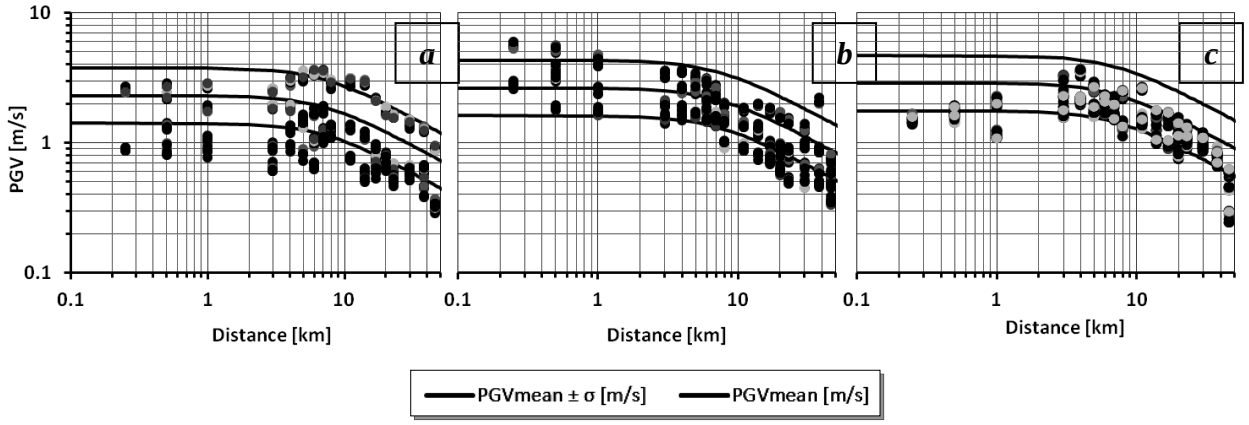


Figure 3. Comparison between the empirical near-source attenuation law by Bray & Rodriguez Marek (2004) and the performed 3D numerical simulations for different source models and associated magnitude: (a) Case 1 ($M_W$ = 5.5), (b) Case 2 ($M_W$ = 6.25), (c) Case 3 ($M_W$ = 6.5).

In Figure 3 the comparison has been carried out in terms of PGV since most of the empirical attenuation laws for near-source propagation have been suitably expressed in this way. This choice turns also useful from the point of view of the numerical computation: a 3D modelization containing both the source and the site of interest requires very long computational time. It is thus necessary to use a less refined discretization of the overall domain. Velocity time-histories, indeed, are less affected by high frequency cut-off due to mesh discretization.

***Effects on large embankments***

After analyzing the ground motion in free-field conditions, large embankments were placed on the free surface of the deposit. To account for the relative distance between the site (embankment) and the source (fault), the embankment location was varied (green points in Figures 1 and 4), with the fault in a fixed position. Among all possible combinations of source and embankments, two cases were selected, corresponding to a dam placed close to the source (Figure 4a) or far from it (Figure 4b). For each embankment the time-histories relative to the points indicated in Figure 5 were analysed. With the letters are represented points on the ground level sufficiently far from the embankments to consider free-field motion. With the numbers are indicated, instead, monitoring points on the external boundaries of the embankment (top and shells) for two embankments of the same height (h = 50m), one located in the vicinity of the fault (near-source) and another far enough from it (far-source). As expected, the accelerations at the base of the embankment placed close to the source (Figure 6a) are much higher than those computed at the base of the embankment in far-source condition (Figure 6b). Evident is the

asynchronism of the accelerograms exciting the embankment base in the x-direction (but the same statement is valid for the y and z components too). For the embankment subjected to the near-source seismic propagation (Figure 6a), also the vertical displacements are much higher (1 order of magnitude) than those induced in the same embankment placed far-source, with a strong variability along the longitudinal axis, as previously observed for the base acceleration.

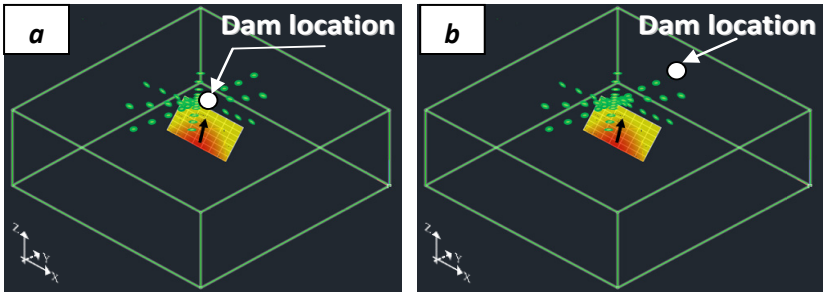


Figure 4. Embankment location: (a) near-source; (b) far-source.

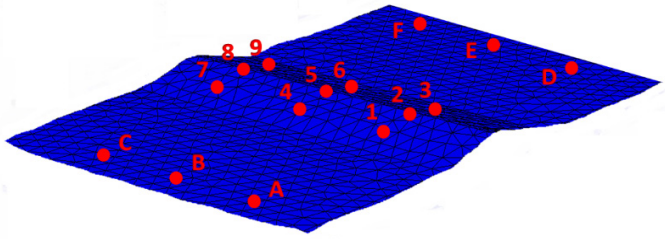


Figure 5. Monitoring points along the ground surface of the deposit (letters from A to F) and along the dam boundary (numbers from 1 to 9).

From the contour of vertical displacements (at a fixed time) for the near-source embankment, it emerges a high spatial variability with respect to the same embankment placed outside the near-source zone. This implies that earth dams placed close to active faults may suffer higher differential settlements to which dangerous cracking phenomena of the embankment body may be related.

## Conclusions

To evaluate the influence of seismic motion variability at the base of large embankments in near-source conditions, a parametric study was performed in which the embankment position with respect to the fault was progressively changed. The source is part of the developed numerical model. The parametric analyses provide evidence that in near-source conditions it is not correct to assume a unique seismic motion at the base of a large embankment (as is usually done for structures placed at considerable distances from the source). Accelerograms calculated at the base of the embankment clearly show a phenomenon of asynchronism (“delay” of the signal with the distance from the source). This phenomenon is of particular relevance in the case of earth dams because of the increased susceptibility to crack formation.

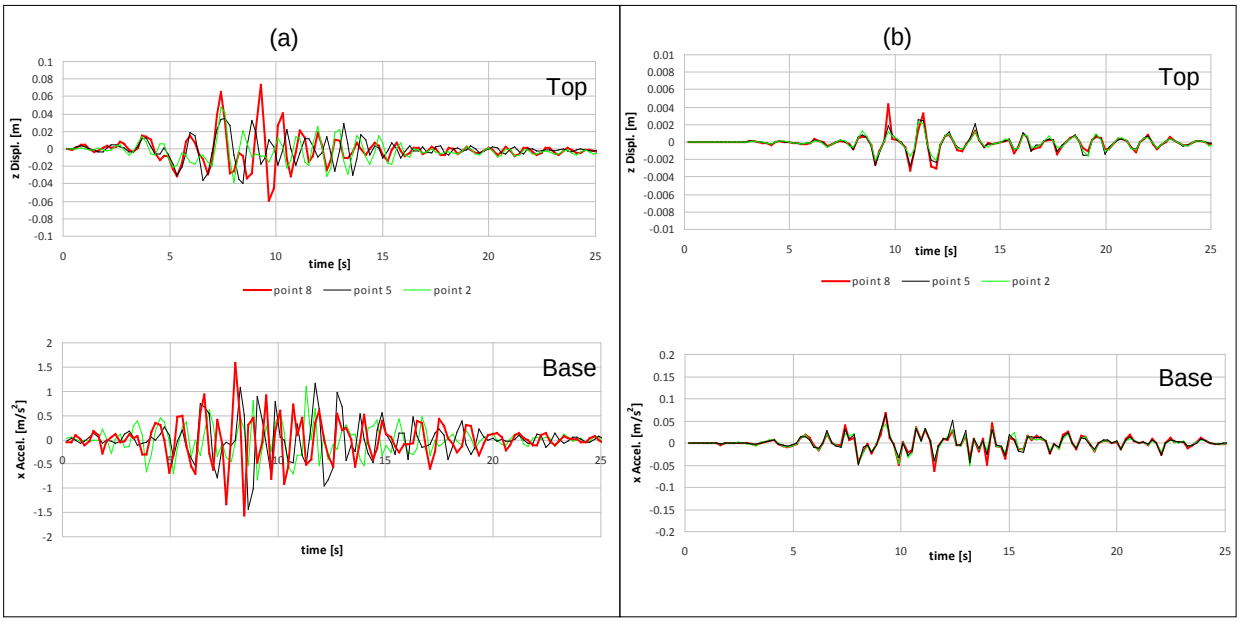


Figure 6. Time histories of vertical displacement for points 2, 5 and 8 placed at the top of the embankment and x-acceleration at the base (same vertical); (a) near-source; (b) far-source.

## Acknowledgments

The reaserch work has been carried out under the auspicious of the Reluis Project 2014-2015, Linea Geotecnica, WP2 (Earth Dams). Coordinators S. Aversa and S. Rampello are kindly acknowledged.

## References

Aki K., Richards P.G. 2002. *Quantitative Seismology*, University Science Books. Sausalito, CA, USA.

Bray J.D., Rodriguez-Marek A. 2004. Characterization of forward-directivity ground motions in the near-fault region. *Soil Dynamics and Earthquake Engineering*; **24**(11):815-828.

Irwin G. 1957. Analysis of stresses and strains near the end of a crack traversing a plate, *Journal of Applied Mechanics*; **24**, 361–364.

Lysmer J., Kuhlemeyer R.L. 1969. Finite dynamic model for infinite media, *J. Eng. Mech. Div.* ASCE, 95, 859-878.

Madariaga R. 1976. Dynamics of expanding circular fault, *Bulletin of the Seismological Society of America* **66**, 639-666.

Somerville P.G. 2005. *Engineering characterization of near fault ground motions.* 2005 NZSEE Conference. Pasadena, CA, USA.

Wells D.L., Coppersmith KJ. 1994. New empirical relationships among magnitude, rupture length, rupture width, rupture area, and surface displacement, *Bull Seism Soc Am*; **84**(4):974-1002.